

---

# VLT / Infrared Integral Field Spectrometer Observations of the Knots in the Planetary Nebula NGC 7293 (the Helix Nebula)

M. Matsuura<sup>1,2</sup>, A.K. Speck<sup>3</sup>, M.D. Smith<sup>4</sup>, A.A. Zijlstra<sup>5</sup>, K.T.E. Lowe<sup>6</sup>, S. Viti<sup>2</sup>,  
M. Redman<sup>7</sup>, C.J. Wareing<sup>5</sup>, and E. Lagadec<sup>5</sup>

<sup>1</sup> National Astronomical Observatory of Japan, Osawa 2-21-1, Mitaka, Tokyo  
181-8588, Japan [mikako@optik.mtk.nao.ac.jp](mailto:mikako@optik.mtk.nao.ac.jp)

<sup>2</sup> Department of Physics and Astronomy, University College London, Gower  
Street, London WC1E 6BT, United Kingdom

<sup>3</sup> Physics and Astronomy, University of Missouri, Columbia, MO 65211, USA

<sup>4</sup> Centre for Astrophysics and Planetary Science, School of Physical Sciences, The  
University of Kent, Canterbury CT2 7NH, United Kingdom

<sup>5</sup> School of Physics and Astronomy, University of Manchester, Sackville Street,  
P.O. Box 88, Manchester M60 1QD, United Kingdom

<sup>6</sup> Science and Technology Research Centre, University of Hertfordshire, College  
Lane, Hatfield, Hertfordshire AL10 9AB, United Kingdom

<sup>7</sup> Department of Physics, National University of Ireland Galway, Galway, Republic  
of Ireland

**Summary.** Knots are commonly found in nearby planetary nebulae (PNe) and star forming regions. Within PNe, knots are often found to be associated with the brightest parts of the nebulae and understanding the physics involved in knots may reveal the processes dominating in PNe. As one of the closest PNe, the Helix Nebula (NGC 7293) is an ideal target to study such small-scale ( $\sim 300$  AU) structures. We have obtained infrared integral-field spectroscopy of a comet-shaped knot in the Helix Nebula using SINFONI on the Very Large Telescope at high spatial resolution (125 mas). With spatially resolved  $2\ \mu\text{m}$  spectra, we find that the  $\text{H}_2$  rotational temperature within the cometary knots is uniform whereas the vibrational temperature decreases towards the tail. The rotational temperature of the cometary knot (situated in the innermost region of the nebula, 2.5 arcmin away from the central star), is 1800 K, higher than the temperature seen in the outer regions (5–6 arcmin from the central star) of the nebula (900 K), showing that the rotational temperature varies across the nebula. The obtained intensities are reasonably well fitted with the  $27\ \text{km s}^{-1}$  C-type shock model. The gas excitation can also be reproduced with a PDR model, but this requires an order of magnitude higher UV radiation. Both models have limitations, highlighting the need for models that treat both hydrodynamics and the PDR.

**Key words:** (ISM:) planetary nebulae: individual: NGC 7293 – ISM: jets and outflows – ISM: molecules – (stars:) circumstellar matter – ISM: clouds – Infrared: stars

## 1 Introduction

In recent years it has become clear that knots of dense material are common in nebulae, including both Planetary Nebulae (PNe) (e.g. [20]) and star-forming regions (e.g. [14]). In the best studied PN case, that of the Helix Nebula (NGC 7293), knots in the inner regions have a comet-like shape [21] and are thus known as cometary knots. The Helix nebula is estimated to contain more than 20,000 cometary-shaped knots [18]. The apparent commonality of occurrence in PNe of these knots has led to the assertion that all circumstellar nebulae are clumpy in structure (e.g. [20, 25, 13]). As knots occupy the brightest parts of the planetary nebulae, understanding their physical nature is essential to understanding the dominant physics governing the nebula.

In addition to being seen as inhomogeneities within the ionized gas emission from nebulae, the knots also contain molecular gas [25, 26]. The excitation mechanisms for molecular hydrogen in planetary nebula have long been controversial, with contention between fluorescent/thermal excitation in photon-dominant regions (PDR) or shock excitation. [28] and [3] showed that vibrationally excited  $H_2$  (by FUV pumping) traces the surface of dense regions in the process of becoming photo-ionized. On the other hand, molecules can form in a post-shock region [19], and  $H_2$  can be excited by shocks [1, 10]. A comparison of models with spatially resolved spectra, which covers multiple line ratios, will help understanding the excitation mechanism of  $H_2$ .

The Helix Nebula (NGC 7293) is one of the nearest PNe, with a largest diameter of more than half a degree [11] and a parallax distance of 219 pc [9]. Because of its distance, small-scale structures inside the nebula are resolved well and this nebula is used as a proxy to understand the structures found in PNe.

## 2 Observations and Analysis

A knot in the Helix Nebula was observed by the Spectrograph for Integral Field Observations in the Near Infrared (SINFONI) [6] installed at the Cassegrain focus of the Very Large Telescope. A concept of the Integral Field Unit (IFU) is demonstrated in Fig. 1; a slicer unit splits the field of view into individual spatial elements which are passed to the spectrometer. We used the grating for the K-band and the spectral resolution  $\lambda/\Delta\lambda$  is 4490. The spatial resolution of the instrument is  $125 \times 250 \text{ mas}^2$ . After the data reduction with GASGANO, the final pixel was re-sampled to a 125 mas scale plate scale image.

The coordinates of our target knot K1 are 22:29:33.414,  $-20:48:04.73$  (J2000). This knot is about 2.5 arcmin away from the central star (Fig. 2). The knot is located at the inner rim of the ring-shaped nebula filled with cometary knots. A nearby star (RA=22:29:33.017 Dec= $-20:48:12.68$ ) was used as Adaptive Optics (AO) guide star. [15] describes the details of the observations and the analysis.

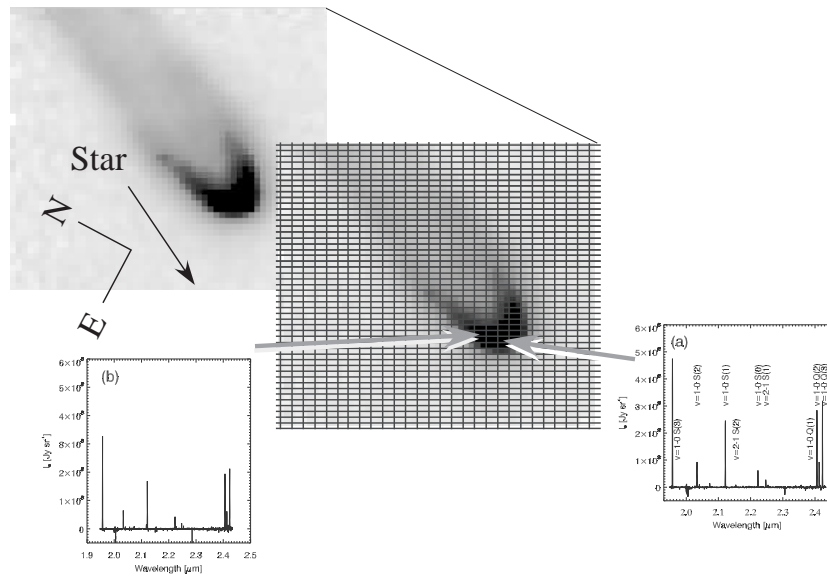


**Fig. 1.** A demonstration of integral field unit observations. A spectrum is obtained at each element, and image at specific wavelength is reconstructed by combining information of all of the elements.

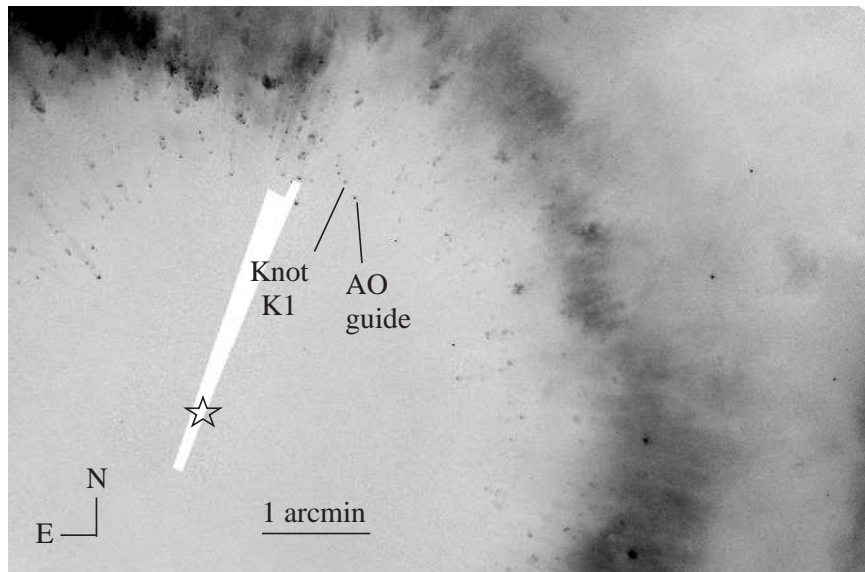


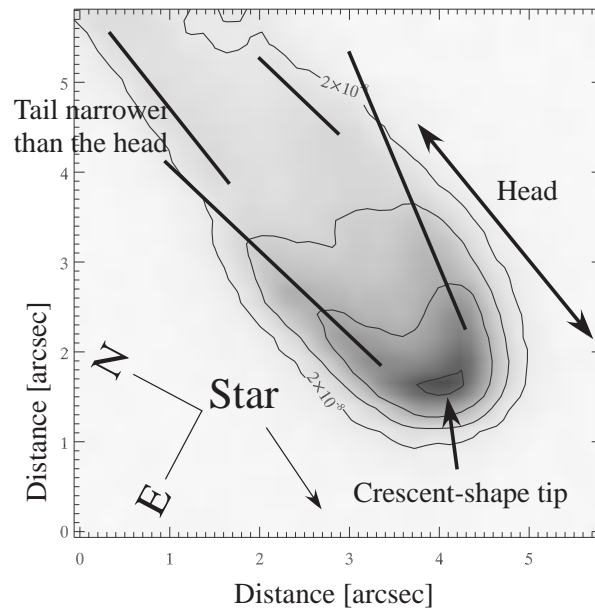
**Fig. 2.** The location of the cometary knot K1 is plotted on the F658N ( $[\text{NII}] + \text{H}\alpha$ ) image [23], together with the AO guide star. The star symbol indicates the place of the central star.

### 3 Description of the data

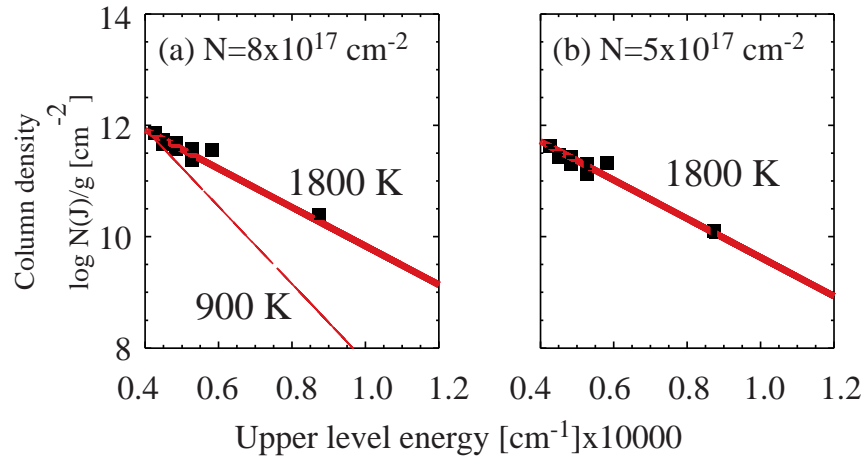
Fig. 3 shows the image of the cometary knot K1 as seen in  $2.12 \mu\text{m}$   $\text{H}_2$  line. The knot shows an elliptical head with a narrower tail. The brightest emission is found in a crescent near the tip of the head. The crescent ends in two linear segments, indicated by the lines in Fig. 3. These segments are not co-aligned and deviate from the direction of the narrower tail. Overall, this gives the impression of a ‘tad-pole’ shape.

Fig. 1 shows example spectra. At most twelve  $\text{H}_2$  lines (three of them with low signal-to-noise ratio) are detected by SINFONI. The  $\text{Br}\gamma$  line is not detected.

Fig. 4 shows the energy diagram of the  $\text{H}_2$  lines at the tip of the knot and at 1 arcsec away from the tip. The slopes in the diagrams show that the line intensities follow an  $T = 1800 \text{ K}$  Local Thermodynamic Equilibrium (LTE) distribution. [15] shows that the temperature remain constant from the head to the tail throughout the knot.



**Fig. 3.** An image of the knot at  $2.12 \mu\text{m}$   $\text{H}_2$   $v=1-0$   $S(1)$  line. The shape of the knot is a tadpole, i.e., a head with a tail which is narrower than the head. The brightest place is found in crescent-shape tip. The contour shows the surface brightness of  $2.12 \mu\text{m}$   $\text{H}_2$   $v=1-0$   $S(1)$  line at  $0.2 \times 10^{-7}$ ,  $0.5 \times 10^{-7}$ ,  $1 \times 10^{-7}$ ,  $2 \times 10^{-7} \text{ W m}^{-2} \text{ sr}^{-1}$ .



**Fig. 4.** The energy diagrams at the brightest tip (a) and at  $\sim 1$  arcsec away from the tip (b). The thick lines show the LTE case for 1800 K and the column densities are indicated in the figure. For a comparison, we plot the 900 K LTE line, as derived for H<sub>2</sub> lines detected in the outer region of the nebula [5]

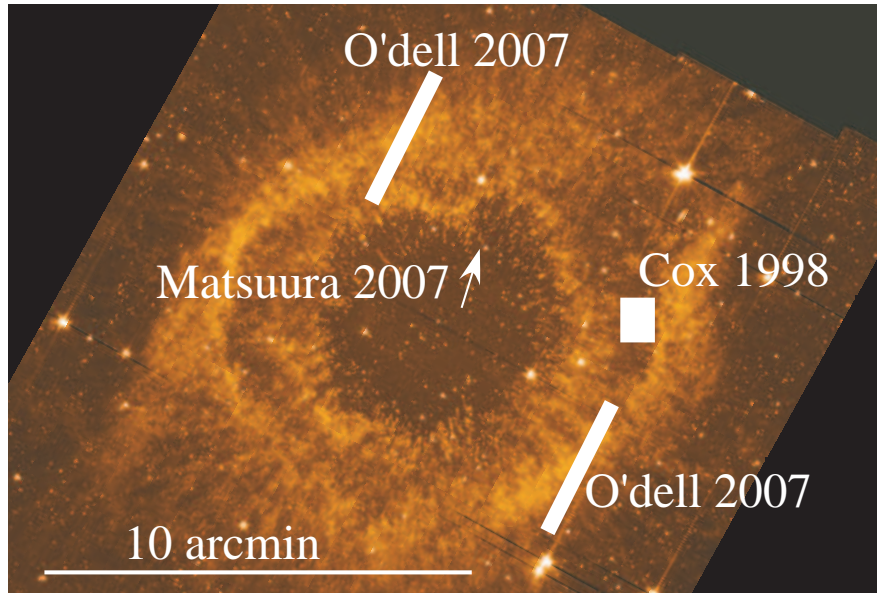


**Fig. 5.** Slit (pixel) positions of H<sub>2</sub> spectroscopic observations and H<sub>2</sub> excitation temperatures

**Table 1.** Intensities of H<sub>2</sub> lines at area (a)–(c) and ratios with respect to the v=2–1 S(1) line. The line ratios are compared with those predicted with a C-type shock model by [12]

Wav $\mu\text{m}$	Transition	Obs ratio	Prd ratio <sup>2</sup>
1.958	v=1–0 S(3) <sup>†</sup>	220	91
2.034	v=1–0 S(2)	36	36
2.073	v=2–1 S(3)	4	
2.128	v=1–0 S(1)	100	100
2.154	v=2–1 S(2)	3	
2.224	v=1–0 S(0)	22	22
2.248	v=2–1 S(1)	9	
2.407	v=1–0 Q(1) <sup>†</sup>	99	75
2.413	v=1–0 Q(2) <sup>†</sup>	29	24
2.424	v=1–0 Q(3) <sup>†</sup>	99	70
2.438	v=1–0 Q(4) <sup>†</sup>	30	20

<sup>1</sup>Line ratio with respect to 2.128  $\mu\text{m}$  v=1–0 S(1) line

<sup>2</sup>Theoretical line ratio from [12]

<sup>†</sup>These lines have a large ( $\sim 30\%$ ) error in relative intensity calibration due to the influence of H<sub>2</sub>O in the terrestrial atmosphere. They are excluded from the comparison with models.

<sup>‡</sup> Marginal detections

## 4 Discussion

### 4.1 Excitation diagrams and temperatures

The H<sub>2</sub> excitation diagrams are fitted by a single LTE temperature of 1800 K. This is much higher than [5] who obtained 900 K by fitting pure-rotational lines up to the S(7) transition. The region where [5] observed is located at the western rim of the nebula, and is 5–6 arcmin away from the central star (Fig. 5). The pixel size of their ISOCAM data was 6 arcsec and emission from multiple knots contributed to each single pixel. In contrast, our target is a single, isolated knot located at the innermost region of the flock of knots (2.5 arcmin from the central star). [22] also obtained an excitation temperature of 988 K from 5–15  $\mu\text{m}$  spectra in the outer part of the nebula. Their two slit positions are 5.6 and 4.2 arcmin from the central star, and the slit size is  $3.6 \times 57 \text{ arcsec}^2$ .

The difference in measured temperatures shows that the excitation temperature of H<sub>2</sub> is not uniform within the Helix nebula, although a careful understanding of different H<sub>2</sub> transitions is required. The H<sub>2</sub> molecules reach higher temperature within the inner region (Fig. 5). From about 2.5 arcmin to 5 arcmin away from the central star, the excitation temperature decreases from 1800 K to 900–1000 K. This provides evidence for temperature variations within the nebula.

## 4.2 Excitation mechanisms of molecular hydrogen

The line intensity ratio is compared with theoretical works. The cometary knot K1 emits a  $2.12\ \mu\text{m}$  1-0 S(1) line intensity of  $2 \times 10^{-7}\ \text{W m}^{-2}\ \text{sterad}^{-1}$ . The adopted uncertainty is a factor of two. The 2-1/1-0 S(1) line ratio is  $\sim 0.1 \pm 0.02$  at the tip.

[4] calculated line intensities of 1-0 S(1) and 2-1 S(1) lines for J-type shocks, C-type shocks and PDR models. The measured line intensities and ratios can be fit equally well under several model conditions.

The speed of ambient gas for C-type shocks is  $v_s \sim 27\ \text{km s}^{-1}$  to fit the H<sub>2</sub> line intensities and line ratios, from theoretical work by [4]. [12] further gave the predicted line ratio for other lines, which are compared with observed ones in Table 1. The predicted and observed line ratios are well consistent. Within an expanding nebula, hydrodynamic effects will cause significant velocity gradients [24], as are observed in PNe [7]. [16, 17] postulate turbulent velocities  $\geq 10\ \text{km s}^{-1}$  (i.e. larger than the sound speed). A C-type shock velocity could be associated with such motion.

PDR may be possible, but increase of UV radiation field is required. The FUV (6–13.6 eV) flux at the knot K1 is about  $G_0 = 8$ , where  $G_0$  is the FUV radiation measured in units of the [8] flux. This is based on [27]'s estimate based on a luminosity of the central star of  $76 L_\odot$  and a distance of 219 pc. The required UV radiation in [4]'s model is  $G_0 > 1 \times 10^4$ , which is an order of magnitude higher than the estimated UV radiation field strength at the knot K1. A similar results are obtained with independent PDR model developed at UCL [2].

In conclusion, among the existing models, shocks can reproduce line intensities but higher velocity than the known wind speed is required. PDR models have difficulty in reproducing the high observed temperature at the local density, and require a drastic increase in the the UV radiation strength. The existence of a PDR region is not in doubt, but it may not contribute significantly to the H<sub>2</sub> excitation in the knot K1. Both models have limitations, highlighting the need for models that treats both hydrodynamics and the PDR.

## References

1. Beckwith S., Neugebauer G., Becklin E.E., Matthews K., Persson S.E., 1980, AJ 85, 886
2. Bell T.A., Viti S., Williams D.A., Crawford I.A., Price R.J., 2005, MNRAS 357, 961
3. Black J.H., van Dishoeck E.F., 1987, ApJ 322, 412
4. Burton M.G., Hollenbach D.J., Tielens A.G.G., 1992, ApJ 399, 563
5. Cox P., Boulanger F., Huggins P.J., et al., 1998, ApJ 495, L23
6. Eisenhauer F., Abuter R., Bickert K., et al. 2003, SPIE 4841, 1548
7. Gesicki K., Acker A., Zijlstra A.A., 2003, A&A, 400, 957
8. Habing H.J., 1968, Bull. Astr. Inst. Netherlands, 19, 421
9. Harris H. C., et al. 2007, AJ, 133, 631
10. Hollenbach D., McKee C.F., 1989, ApJ 342, 306
11. Hora J.L., Latter W.B., Smith H.A., Marengo M., 2006, ApJ 652, 426
12. Kaufman M.J., Neufeld D.A., 1996, ApJ 456, 611
13. Matsuura M., Zijlstra A.A., Molster F.J., Waters L.B.F.M., Nomura H., Sahai R., Hoare M.G., 2005b, MNRAS 359, 383

14. McCaughrean M.J., Mac Low M.-M., 1997, AJ 113, 391
15. Matsuura M., Speck A.K., Smith M.D., et al. accepted for publication in MNRAS (astro-ph/07093093)
16. Meaburn J., Clayton C.A., Bryce M., Walsh J.R., Holloway A.J., Steffen W., 1998, MNRAS 294, 201
17. Meaburn J., Boumis P., López, J.A., Harman D.J., Bryce M., Redman M.P., Mavromatakis F., 2005, MNRAS 360, 963
18. Meixner M., McCullough P., Hartman J., Son M., Speck A., 2005, AJ 130, 1784
19. Neufeld D.A., Dalgarno A., 1989, ApJ 340, 869
20. O'Dell C. R., Balick B., Hajian A. R., Henney W. J., & Burkert A. 2002, AJ, 123, 3329
21. O'Dell C.R., Handron K.D., 1996, AJ 111, 1630
22. O'Dell C.R., Henney W.J., Ferland G.J., 2007, AJ, 133, 2343
23. O'Dell C.R., McCullough P.R., Meixner M., 2004, AJ 128, 2339
24. Schoenberner D., Jacob R., Steffen M. 2005, A&A 441, 573
25. Speck A.K., Meixner M., Fong D., McCullough P.R., Moser D.E., Ueta T., 2002, AJ 123, 346
26. Speck A.K., Meixner M., Jacoby G.H., Knezek P.M., 2003, PASP 115, 170
27. Su K.Y.L., Chu Y.-H., Rieke G.H., et al., 2007 2007, ApJ 657, L41
28. Tielens A.G.G.M., Hollenbach D., 1985, ApJ 291, 747